Oxidation state governs structural transitions in peroxiredoxin II that correlate with cell cycle arrest and recovery

Timothy J. Phalen,[1] Kelly Weirather,[1] Paula B. Deming,[2] Vikas Anathy,[1] Alan K. Howe,[2] Albert van der Vliet,[1] Thomas J. Jönsson,[3] Leslie B. Poole,[3] and Nicholas H. Heintz[1]

[1]Department of Pathology and [2]Department of Pharmacology, University of Vermont College of Medicine, Burlington, VT 05405
[3]Center for Structural Biology, Wake Forest University School of Medicine, Winston-Salem, NC 27157

Inactivation of eukaryotic 2-Cys peroxiredoxins (Prxs) by hyperoxidation has been proposed to promote accumulation of hydrogen peroxide (H_2O_2) for redox-dependent signaling events. We examined the oxidation and oligomeric states of PrxI and -II in epithelial cells during mitogenic signaling and in response to fluxes of H_2O_2. During normal mitogenic signaling, hyperoxidation of PrxI and -II was not detected. In contrast, H_2O_2-dependent cell cycle arrest was correlated with hyperoxidation of PrxII, which resulted in quantitative recruitment of ~66- and ~140-kD PrxII complexes into large filamentous oligomers. Expression of cyclin D1 and cell proliferation did not resume until PrxII-SO_2H was reduced and native PrxII complexes were regenerated. Ectopic expression of PrxI or -II increased Prx-SO_2H levels in response to oxidant exposure and failed to protect cells from arrest. We propose a model in which Prxs function as peroxide dosimeters in subcellular processes that involve redox cycling, with hyperoxidation controlling structural transitions that alert cells of perturbations in peroxide homeostasis.

Introduction

Reentry into the cell cycle requires integration of signals from several redox-dependent processes (Burch and Heintz, 2005). For example, production of hydrogen peroxide (H_2O_2) is required for mitogenic signaling in response to EGF, bFGF, PDGF, and thrombospondin2 (Gabbita et al., 2000; Karin and Shaulian, 2001). One mechanism by which H_2O_2 acts in mitogenic signaling is through the transient oxidation of cysteine residues present in signaling targets such as the phosphatases protein tyrosine phosphatase 1B and PTEN (phosphatase and tensin homologue on chromosome 10), which regulate signaling through the extracellular signal–related kinase (ERK) 1/2 and PI3-kinase–Akt pathways, respectively (for review see Forman et al., 2004).

Given the prominent role of oxidants in cell cycle reentry, the G0–G1 transition can be considered an oxidative phase of the cell cycle, as suggested by a recent study on metabolic cycles in yeast (Tu et al., 2005). However, although production of H_2O_2 in response to growth factors is required for cell cycle reentry (Finkel, 2003), high levels of H_2O_2 during the G0–G1 transition cause cell cycle arrest. In serum-stimulated mouse lung epithelial cells, as in many other cell types (for review see Schwartz and Assoian, 2001), signals from the ERK1/2 and PI3-kinase–Akt pathways are integrated temporally at the level of expression of cyclin D1 (Yuan et al., 2003, 2004; Burch et al., 2004). Recently, we showed that pathways regulating expression of cyclin D1 are targeted by reactive oxygen species (ROS) and reactive nitrogen species, resulting in cell cycle arrest (Yuan et al., 2003, 2004; Burch et al., 2004). Arrest can be bypassed by loading cells with catalase (Yuan et al., 2003), supporting the notion that intracellular levels of H_2O_2 represent one mechanism for redox-dependent control of cell cycle progression.

Peroxiredoxins (Prxs) are a highly abundant family of widely expressed antioxidant enzymes (for reviews see Wood et al., 2003b; Immenschuh and Baumgart-Vogt, 2005; Rhee et al., 2005). Because PrxI interacts with c-Abl (Wen and Van Etten, 1997) and c-Myc (Mu et al., 2002; Egler et al., 2005) and PrxII modulates signaling through the PDGF receptor (Choi et al., 2005), Prxs have emerged as important factors that link ROS metabolism to redox-dependent signaling events. All Prxs use a redox-active peroxidatic cysteine to attack peroxide substrates, resulting in the formation of a cysteine sulfenic acid (Cys-SOH). As is typical for 2-Cys Prxs, PrxI and -II are obligate

Correspondence to Nicholas H. Heintz: nicholas.heintz@uvm.edu

Abbreviations used in this paper: DNCB, 1-chloro-2,4-dinitrobenzene; ERK, extracellular signal–related kinase; GOx, glucose oxidase; GSH, glutathione; HMC, high molecular mass complex; Prx, peroxiredoxin; ROS, reactive oxygen species; Trx, thioredoxin; TrxR, thioredoxin reductase.

© The Rockefeller University Press $8.00
The Journal of Cell Biology, Vol. 175, No. 5, December 4, 2006 779–789
http://www.jcb.org/cgi/doi/10.1083/jcb.200606005

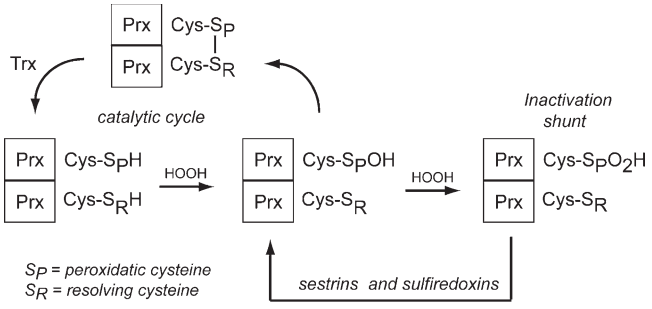

Figure 1. **The catalytic cycle of C-Cys eukaryotic Prxs.** (A) When exposed to H_2O_2, the peroxidatic cysteine (S_PH) of 2-Cys Prxs is oxidized to sulfenic acid (Prx-SOH). Upon reaction with the resolving cysteine (S_RH), a Prx dimer with an intermolecular disulfide bond is formed, which is then reduced by Trx to regenerate active enzyme. Because of a pause in the catalytic cycle, the S_PH of eukaryotic 2-Cys Prxs is susceptible to hyperoxidation, resulting in the formation of a sulfinic acid form (Prx-SO_2H) that is catalytically inactive. Sulfiredoxins and sestrins are ATP-dependent sulfinyl reductases that participate in retroreduction of Prx-SO_2H, regenerating active enzyme. 2-Cys Prxs are obligate homodimers that can assemble into decamers and higher molecular mass oligomers, depending on oxidation state, pH, calcium concentrations, and posttranslational modifications such as phosphorylation.

homodimers, and in these enzymes the Cys-SOH of the peroxidatic cysteine in one subunit is attacked by a resolving cysteine in the neighboring subunit, resulting in an intersubunit disulfide bond. In mammalian cells, the intersubunit disulfide is reduced by thioredoxin (Trx), which is then regenerated by Trx reductase (TrxR) using reducing equivalents from NAD(P)H (Fig. 1). Calcium concentration, pH, and oxidation state influence the assembly of 2-Cys Prx dimers into decamers, and decamers into high molecular mass oligomers (for reviews see Wood et al., 2003b; Immenschuh and Baumgart-Vogt, 2005; Rhee et al., 2005). Recent work also provides evidence for a link between structural transitions in the oligomeric state of Prxs and their peroxidase and protein chaperone activities (Wood et al., 2003a; Parsonage et al., 2005; Jang et al., 2006).

In contrast to prokaryotic homologues, eukaryotic 2-Cys Prxs have a particularly interesting biochemical characteristic in that they are readily inactivated by their own substrate, H_2O_2. Because of a C-terminal domain that induces a kinetic pause in the catalytic cycle, the peroxidatic cysteine of PrxI and -II is susceptible to hyperoxidation, leading to the formation of sulfinic acid (Cys-SO_2H), which cannot participate in disulfide bond formation with the resolving cysteine (Wood et al., 2003a). Inactivation through hyperoxidation has been proposed to allow H_2O_2 to accumulate to substantial levels, thereby facilitating redox-dependent signaling, a concept known as the "floodgate" hypothesis (Wood et al., 2003a). The fact that the sulfinic acid form of 2-Cys Prxs is not a terminal end product but can be reduced in an ATP-dependent manner by sulfinyl reductases, such as sulfiredoxins (Biteau et al., 2003; Chang et al., 2004) and p53-inducible sestrins (Budanov et al., 2004), suggests that Prx-SO_2H may participate in regulatory signaling loops.

We tested the relevance of the floodgate hypothesis during mitogenesis by investigating the connection between the oxidative state of Prx isoforms and cell cycle entry and arrest. Our studies indicate that widespread inactivation of PrxI and -II by hyperoxidation is not a facet of normal mitogenic signaling. Rather, examination of dose-dependent responses to fluxes of H_2O_2 demonstrate that cell cycle arrest in response to oxidative stress correlates with recruitment of PrxII-SO_2H into cytoplasmic oligomers and that recovery of cell proliferation occurs after Prx-SO_2H is reduced. Unexpectedly, transient overexpression of PrxI and -II led to increased levels of hyperoxidized Prxs in response to oxidative stress and failed to protect cells from arrest. We propose that Prx-SO_2H functions in stress response pathways that warn cells of perturbations in oxidant metabolism and thereby contribute to oxidant-induced cell cycle arrest.

Results

Effects of H_2O_2 on mitogenic signaling

To examine the oxidation state of Prxs during mitogenic signaling, mouse C10 lung epithelial cells were collected in G0 by serum deprivation, and the formation of Prx-SO_2H in response to serum stimulation was assessed using an antibody specific for Prx-SO_2H. Prx-SO_2H was not detected above background levels in cells stimulated for 15 min with medium containing serum concentrations from 2 to 20%, a range that induces dose-dependent induction of tyrosine phosphorylation (Fig. 2 A, lanes 2–5), activation of the ERK1/2 and PI-3 kinase–Akt mitogenic signaling pathways, and expression of cyclin D1 (Ranjan et al., 2006). These results indicate that normal mitogenic signaling does not require inactivation of Prxs by hyperoxidation, in agreement with a recent report on the role of PrxII in PDGF signaling (Choi et al., 2005).

To further explore Prx oxidation in cell cycle control, we adopted an experimental paradigm that utilizes a dose-dependent H_2O_2 generating system to evoke transient cell cycle arrest (Burch et al., 2004). C10 cells were synchronized in G0 by serum deprivation and induced to reenter the cell cycle by adding medium containing 10% FBS with or without glucose oxidase (GOx). In complete medium with glucose and 10% FBS, GOx caused the dose-dependent production of H_2O_2 in a linear fashion for at least 8 h (Fig. 2 B). For example, in complete medium, 5.0 mU/ml GOx generated $\sim$10 μM H_2O_2/h.

During the first 6 h of serum stimulation, 1.0 or 2.5 mU/ml GOx had little effect on the expression of cyclin D1, whereas doses of 5.0 mU/ml or greater blocked expression of cyclin D1 (Fig. 2 C, lanes 7–9). In response to continuous exposure to 1.0 mU/ml GOx, the levels of activated ERK1/2 were similar to the serum control, cyclin D1 was expressed, and hyperoxidized 2-Cys Prxs were not observed (Fig. 2 C, lane 5), suggesting that C10 cells are able to metabolize considerable amounts of exogenous H_2O_2 during the G0–G1 transition without accumulating hyperoxidized 2-Cys Prxs. At 2.5 mU/ml, levels of phospho-ERK1/2 were unaffected, Prx-SO_2H was barely detectable after 6 h of exposure, and cyclin D1 was expressed at nearly normal levels. In contrast, at 5.0 mU/ml, hyperoxidized Prx-SO_2H accumulated to substantial levels and cyclin D1 was not expressed (Fig. 2 C, lane 7). Concentrations of GOx $\geq$10.0 mU/ml induced accumulation of hyperoxidized Prx-SO_2H, caused hyperactivation of ERK1/2, and blocked expression of cyclin D1 (Fig. 2 C, lanes 8 and 9).

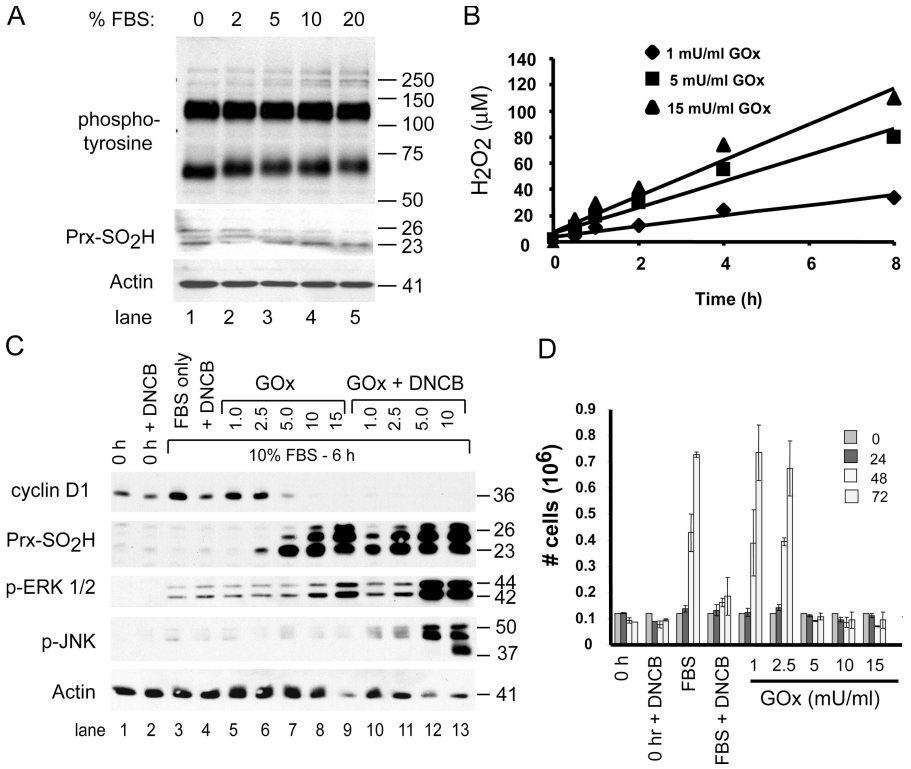

Figure 2. **Hyperoxidation of Prxs in serum-stimulated cells correlates with inhibition of cell proliferation.** (A) C10 cells synchronized by serum deprivation were stimulated with medium containing the indicated concentration of FBS for 15 min, and levels of phosphotyrosine and Prx-SO_2H were assessed by immunoblotting. Actin was used as a loading control. (B) For generating fluxes of H_2O_2, GOx was added to DME with 10% FBS at the indicated concentration, and the amount of H_2O_2 in medium was measured as a function of time. (C) Serum-starved mouse lung epithelial (C10) cells (time 0) were stimulated with DME containing 10% FBS and the indicated concentrations of GOx (mU/ml), with or without 5 μM DNCB, for 6 h. Cell extracts were examined for expression of the indicated proteins by immunoblotting. PrxI and -II comigrate under reducing conditions on SDS gels; based on molecular mass, the band at 26 kD is mitochondrial PrxIII. (D) The indicated concentrations of GOx were added to culture medium during serum stimulation, and replicate C10 cultures were counted over a 3-d period to assess cell proliferation. Control cultures (time 0) were maintained in DME with 0.5% FBS for the duration of the experiment or stimulated with 10% FBS alone. Error bars indicate mean ± SD.

We previously showed that termination of ERK1/2 signaling after 3 h of exposure to the highest dose of GOx (15 mU/ml) restores expression of cyclin D1 but not cell proliferation (Burch et al., 2004). Hence, prolonged activation of ERK1/2 is a useful marker of oxidant-induced arrest at the G0–G1 transition of the cell cycle. Although GOx influenced the levels of phospho-ERK1/2 in a dose-dependent manner as before, it did not induce phosphorylation of JNK in synchronized cells at any dose (Fig. 2 C, lanes 5–9). In asynchronous cells, activation of JNK in C10 cells by H_2O_2 is associated with cell death (Pantano et al., 2003).

To determine if retroreduction of Prx-SO_2H prevented the accumulation of Prx-SO_2H, serum-stimulated cells were treated with 1-chloro-2,4-dinitrobenzene (DNCB), with or with out GOx. DNCB depletes cells of reduced glutathione (GSH) and blocks reduction of Trx by inhibiting TrxR (Arner et al., 1995), thereby impairing the ability of Trx and GSH to participate in the retroreduction of Prx-SO_2H to catalytically active forms. Within 10 min, 5 μM DNCB caused a 90% reduction in GSH levels that persisted for at least 3 h (unpublished data).

In the absence of GOx, DNCB blocked the ability of serum to induce expression of cyclin D1 but did not prevent phosphorylation of ERK1/2 (Fig. 2 C, lane 4) or cause the accumulation of hyperoxidized Prxs. In contrast, DNCB markedly sensitized 2-Cys Prxs to hyperoxidation by GOx (Fig. 2 C, compare lanes 6–9 with lanes 10–13), suggesting that Prx retroreduction pathways are active during cell cycle reentry. Although phospho-ERK1/2 levels were increased in cells treated with GOx and enhanced in cells treated with DNCB and GOx, only with DNCB were high concentrations of GOx able to induce phosphorylation of JNK (Fig. 2 C, lanes 10–13).

Cell proliferation was then examined in serum-stimulated cells treated with DNCB and/or GOx (Fig. 2 D). GOx and/or DNCB were added to serum-stimulated cells, and proliferation was examined over a 3-d period without changing the culture media. C10 cells exposed to 1.0 or 2.5 mU/ml GOx proliferated as well as untreated controls, whereas those exposed to doses of GOx ≥5.0 mU/ml failed to proliferate by 3 d (Fig. 2 C). Greater than 70% of cells arrested in response to all but the highest dose of GOx (15.0 mU/ml) remained viable for at least 3 d (Fig. 2 D and not depicted). Caspase 3 was not activated in serum-stimulated cells at any dose of GOx, although it was readily activated after exposure to GOx by staurosporin (unpublished data), indicating that proapoptotic pathways were functional in arrested C10 cells. Cells treated with DNCB alone recovered slowly (Fig. 2 D), whereas cells treated with DNCB and any dose of GOx did not proliferate (not depicted).

Although DNCB sensitized Prxs to hyperoxidation by GOx, it did not sensitize Prxs to hyperoxidation in response to serum at any time point. Together, these studies indicate that formation of Prx-SO_2H may not be required for mitogenic signaling during the G0–G1 transition of the cell cycle. In contrast, dose-response experiments with GOx revealed a sharp transition from unimpeded cell proliferation to cell cycle arrest that occurred between concentrations of 2.5 and 5.0 mU/ml, and that arrest was reflected in failure to express cyclin D1.

Oxidation of PrxI and -II and cell cycle progression

Transitions between dimers, decamers, and high molecular mass oligomers of Prxs are governed by oxidation state (Wood et al., 2002; Moon et al., 2005), phosphorylation during G2/M

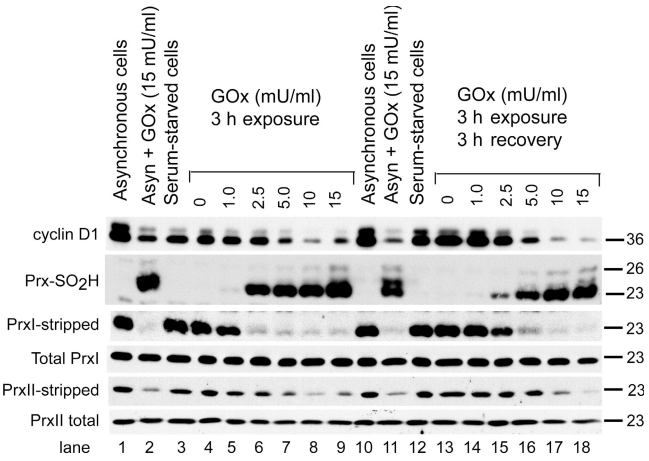

Figure 3. **Dose-dependent hyperoxidation of PrxI and -II by fluxes of hydrogen peroxide.** Serum-starved C10 cells were stimulated with DME with 10% FBS containing the indicated concentration of GOx for 3 h. After exposure, cells were washed and allowed to recover for 3 h in fresh medium. Asynchronous cells plated at the same density in DME with 10% FBS were used as controls. Cell extracts were examined for the expression of cyclin D1, total PrxI, total PrxII, and Prx-SO_2H by standard SDS-PAGE and immunoblotting. Note that cyclin D1 is degraded in response to GOx in asynchronous cells, whereas GOx did not affect the levels of total PrxI and -II under any condition. To assess levels of PrxI and -II that were not hyperoxidized in serum-stimulated cells, immunoblots first probed for Prx-SO_2H were stripped and reprobed for PrxI or -II (see Materials and methods).

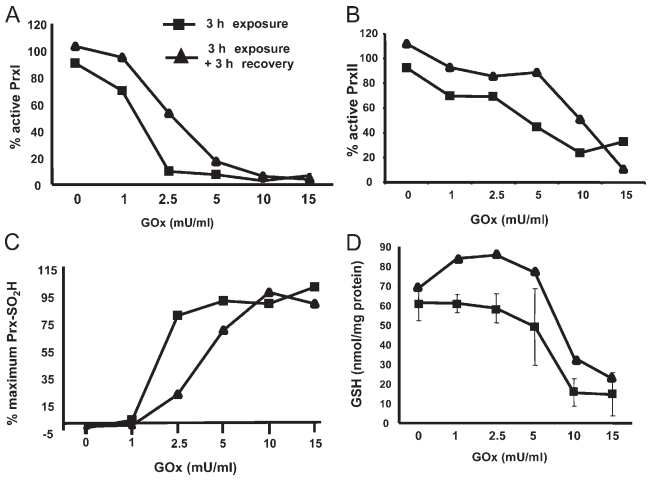

Figure 4. **Prx oxidation occurs before depletion of cellular GSH.** Using the strip–reprobe immunoblotting method, densitometry was used to quantify the signals for the fraction of PrxI (A) or PrxII (B) that was not hyperoxidized as a function of GOx concentration after 3 h of exposure to the indicated concentration of GOx (squares) or after a 3-h recovery period (diamonds). (C) Total Prx-SO_2H levels are expressed as a percentage of the maximal signal obtained with 15 mU/ml GOx, which caused quantitative hyperoxidation of PrxI and -II. (D) Reduced GSH levels were measured in extracts from C10 cells treated with GOx and allowed to recover in the same fashion. Error bars indicate mean ± SD.

(Chang et al., 2002; Jang et al., 2006), and other parameters (for review see Wood et al., 2003b). To study the oxidation state of 2-Cys Prxs under various conditions, an immunoblotting method was devised to detect the relative amounts of reduced or oxidized Prx (Prx-SH, Prx-SOH, or Prx-S-S-Prx) versus hyperoxidized Prx (Prx-SO_2H). With this method, it was possible to estimate the fraction of catalytically active PrxI and -II despite the limitation that the Prx-SO_2H antibody recognizes hyperoxidized PrxI and -II with equivalent efficiency.

When extracts were resolved by standard SDS-PAGE, total PrxI and -II levels detected by immunoblotting and quantified by densitometry varied less than ±8% during the first 6 h after serum stimulation, with or without GOx (Fig. 3). When probed first for Prx-SO_2H and then for either PrxI or -II after stripping the membrane, immunoblotting produced reciprocal signals that reflected the fraction of PrxI or -II that was not catalytically inactivated versus the fraction that was inactivated by hyperoxidation. Using densitometry, the levels of reduced/oxidized PrxI (Fig. 4 A), reduced/oxidized PrxII (Fig. 4 B), and Prx-SO_2H (Fig. 4 C) were estimated as a function of GOx concentration after 3 h of exposure and after 3 h of recovery in fresh medium (Fig. 3). At 2.5 mU GOx/ml, >85% of PrxI was hyperoxidized after a 3-h exposure (Fig. 3, lane 6). After recovery, <50% of PrxI was hyperoxidized, and the reduction in Prx-SO_2H levels (Fig. 4 C) was accompanied by recovery of the signal for reduced PrxI (Fig. 3, lane 15; and Fig. 4 A), confirming the activity of retroreduction pathways in C10 cells. PrxII appeared to be less sensitive to hyperoxidation than PrxI; at 2.5 mU/ml GOx (Fig. 3, lane 6), only ~25% of PrxII had been inactivated by 3 h (Fig. 4 B). At 10 or 15 mU/ml, both PrxI and -II were quantitatively hyperoxidized (Fig. 3 A, compare lanes 8 and 9 with lanes 17 and 18), and little signal for reduced PrxI and -II was regained after a 3-h recovery period (Fig. 4, A and B). In cells treated with GOx, expression of cyclin D1 was inversely correlated with the levels of Prx-SO_2H (Fig. 3).

To assess the relationship between Prx hyperoxidation and cellular redox status, GSH levels were measured as a function of GOx concentration after exposure and recovery (Fig. 4 D). A considerable drop in GSH levels was not observed at 3 h until concentrations of GOx exceeded 5.0 mU/ml, and at all concentrations of GOx, GSH levels increased after recovery in fresh medium (Fig. 4 D). These results agree well with a report that shows PrxII is hyperoxidized in response to levels of H_2O_2 that do not inhibit the TrxR–Trx system or deplete cells of GSH (Baty et al., 2005). Hence, cells treated with 5.0 mU/ml GOx for 3 h that retained near normal levels of GSH underwent transient cell cycle arrest, whereas those treated with either 10 or 15 mU/ml GOx that accumulated hyperoxidized PrxI and -II that could not be reduced after 3 h of recovery (Fig. 3), perhaps because of low GSH levels (Fig. 4 D), were not able to proliferate.

Serum stimulation engages PrxI and -II in peroxide metabolism

When assessed under standard conditions, the total levels of PrxI and -II did not change during the first 6 h of serum stimulation (Fig. 3). When samples were denatured in the presence of SDS, but without reducing agents to preserve disulfide bonds, gel electrophoresis showed that both PrxI (Fig. 5, lane 1) and PrxII (lane 7) from serum-starved cells were partitioned between 23-kD Prx-SH/Prx-SOH monomers and 38-kD Prx-S-S-Prx homodimers. Upon addition of serum, the levels of PrxI (Fig. 5, lanes 2–6) and Prx II (lanes 8–12) monomers decreased,

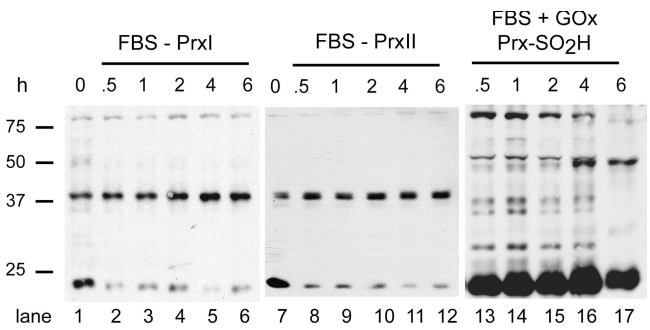

Figure 5. **Serum stimulation increases the levels of Prx-S-S-Prx dimers.** At the indicated times, extracts were prepared from serum-stimulated C10 cells in the absence of reducing agents and resolved by gel electrophoresis in the presence of SDS. After transfer, blots were probed for PrxI or -II as indicated. Extracts from serum-stimulated cultures treated with15 mU/ml GOx were prepared in the same fashion and probed for Prx-SO_2H. Serum-starved cells (time 0) were used as controls.

and PrxI and -II homodimers with intersubunit disulfide bonds increased (Fig. 5, lanes 2–6 and 8–12, respectively). After exposure to 15 mU/ml GOx, all dimers with intersubunit disulfide bonds were lost by 30 min, and only hyperoxidized PrxI and -II monomers were detected for the duration of the experiment (Fig. 5, lanes 13–17; and not depicted). Because homodimers with intersubunit disulfide bonds are produced only during peroxide catalysis (Fig. 1), these results indicate that PrxI and -II metabolize H_2O_2 produced in response to serum stimulation. Upon hyperoxidation, a condition in which intersubunit disulfide bonds cannot form, only Prx-SO_2H monomers were observed, as expected.

Recruitment of hyperoxidized PrxII into high molecular mass oligomers

At 2.5 mU/ml GOx, 85% of PrxI was hyperoxidized, and yet cells expressed cyclin D1 and proliferated normally. In contrast, cells treated with 5.0 mU/ml GOx did not express cyclin D1 or proliferate. To better understand this difference, native gel electrophoresis was used to examine the effect of GOx on the oligomerization state of PrxI and -II. When cell extracts were resolved by electrophoresis in the absence of reducing agents and SDS, immunoblotting indicated that PrxI was organized exclusively in complexes >660 kD (unpublished data). In contrast, PrxII was detected in two sets of bands that we refer to as A–A' and B–B' (Fig. 6). Compared with the mobility of native molecular mass markers, A–A' migrated with an apparent molecular mass of ~66 kD and B–B' with a mass of ~140 kD. Although similar PrxII complexes have been observed in other cell types (Moon et al., 2005), the precise constituents of these complexes are not known.

In extracts of serum-starved cells, bands A and B were the predominant form of PrxII (Fig. 6 A, lane 1). Addition of DNCB or FBS alone for 3 h did not change the mobility of PrxII on native gels (Fig. 6 A, lanes 2 and 3), but together DNCB and FBS increased the signal of band B' (lane 4). Because FBS and DNCB do not induce Prx hyperoxidation (Fig. 3), changes in band B may reflect structural transitions during formation of PrxII-S-S-PrxII dimers during peroxide metabolism (Fig. 5), in

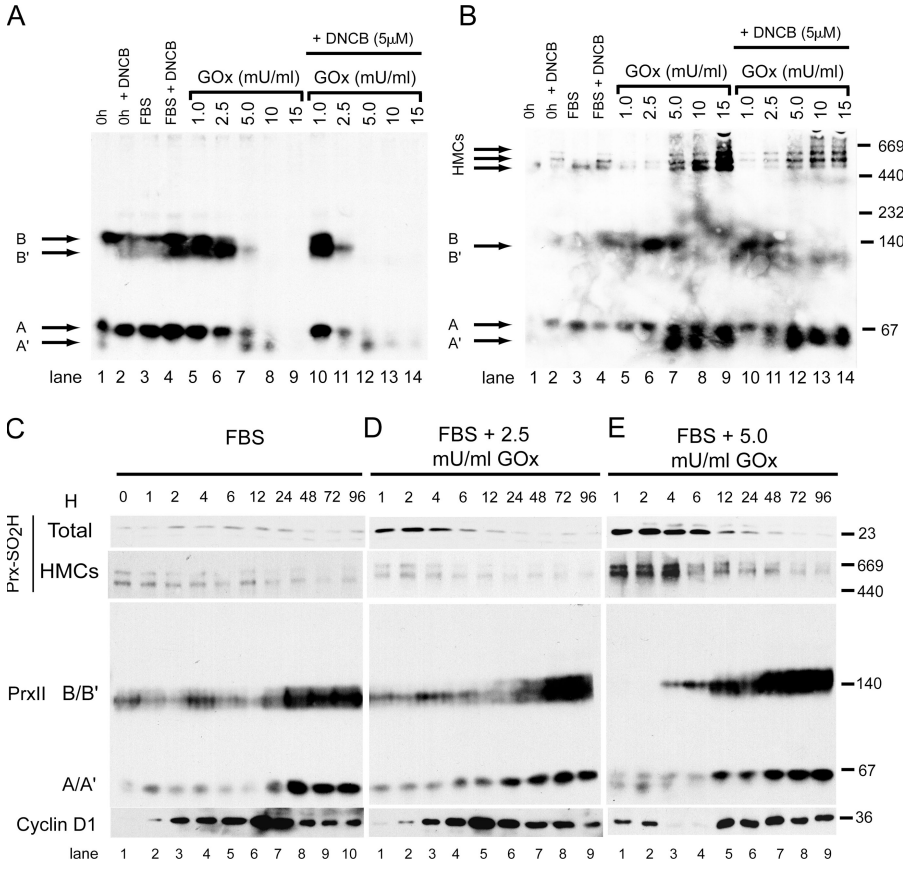

Figure 6. **Hyperoxidation of PrxII induces structural transitions that correlate with cell cycle arrest.** (A and B) Serum-starved C10 cells (time 0) were stimulated with medium containing 10% FBS and the indicated concentration of GOx with or without 5 μM DNCB. Cell extracts prepared in the absence of reducing agents were resolved by native gel electrophoresis to preserve protein complexes. After transfer, immunoblots first were probed for PrxII (A), and after stripping, for Prx-SO_2H (B). Complexes A–A' and B–B' migrated with apparent molecular masses of ~66 and ~140 kD, respectively. HMCs detected by the anti–Prx-SO_2H antibody in B migrated with apparent molecular masses >500 kD. To examine the dynamics of these complexes in response to oxidative stress, extracts were prepared at the indicated times from cells stimulated with FBS alone (C) or from cells stimulated with FBS containing 2.5 mU/ml (D) or 5.0 mU/ml (E) GOx for the first 3 h of serum stimulation. Samples were resolved under reducing conditions for assessing total levels of Prx-SO_2H and cyclin D1 and native conditions for visualizing HMCs and PrxII complexes A–A' and B–B'.

agreement with studies that show PrxII metabolizes H_2O_2 produced in response to growth factors (Choi et al., 2005) and terminates H_2O_2-activated signaling by phospholipase D1 (Xiao et al., 2005).

In response to exposure to 1.0 or 2.5 mU/ml GOx, band B' increased in abundance relative to band B, perhaps reflecting increased engagement of the PrxII 140-kD complex in peroxide metabolism (Fig. 6 A, lanes 5 and 6). At concentrations of GOx of 5.0 mU/ml or higher, bands B and B' disappeared, band A decreased, and band A' appeared (Fig. 6 A, lanes 7–9). As observed in Fig. 3, DNCB shifted the dose response for the A–A' and B–B' complexes to lower concentrations of GOx (Fig. 6 A, lanes 10–14).

When reprobed for Prx-SO_2H, little hyperoxidized PrxII was observed for cells treated with 1.0 mU/ml GOx (Fig. 6 B, lane 5), whereas hyperoxidized Prx-SO_2H was observed to comigrate with band B' in extracts from cells treated with 2.5 mU/ml GOx (Fig. 6 B, lane 6). At concentrations of GOx $\geq$5.0 mU/ml, Prx-SO_2H was incorporated into several discrete high molecular mass complexes (HMCs) with apparent molecular masses >500 kD and considerable levels of A' accumulated (Fig. 6 B, lanes 7–9). Recruitment of Prx-SO_2H into HMCs correlated with loss of signal from the PrxII B–B'complex (Fig. 6 A, lanes 7–9).

PrxII complexes accumulate during cell proliferation

In time course experiments, the A–A' and B–B' complexes responded to serum stimulation and cell proliferation and, during recovery from exposure, to 5.0 mU/ml GOx. The levels of the 140-kD B–B' complex fluctuated during the first 12 h of serum stimulation (Fig. 6 C, lanes 1–6) and increased markedly in abundance as cells reached confluence 48–96 h later (lanes 8–10). As cells reached confluence, increases in the A–A' also were observed (Fig. 6 C, lanes 8–10). Serum stimulation and cell proliferation for >3 d caused no change in the signal for total Prx-SO_2H detected under reducing and denaturing conditions or Prx-SO_2H in HMCs detected by native gel electrophoresis (Fig. 6 C, lanes 2–10). The PrxII complexes were largely unaffected by exposing cells to 2.5 mU/ml GOx for the first 3 h of serum stimulation (Fig. 6 D, lanes 1–9), even though substantial levels of Prx-SO_2H were observed under these conditions (Fig. 6 D, lanes 1–4) and the cultures took slightly longer to reach confluence. Note that 2.5 mU/ml GOx did not increase HMCs containing Prx-SO_2H.

At 5.0 mU/ml GOx, the B–B' complex was not observed during the 3-h exposure, HMCs containing Prx-SO_2H increased in abundance, and cyclin D1 was not expressed (Fig. 6 E, lanes 1 and 2). After GOx was removed at 3 h, total Prx-SO_2H levels were reduced over time, and Prx-SO_2H in HMCs returned to background levels (Fig. 6 E, lanes 3–9). As signal for Prx-SO_2H diminished in HMCs, A' was lost, the B–B' complex reappeared, and cyclin D1 was expressed (Fig. 6 E, lanes 5–9). By 96 h, the HMCs and PrxII A–A' and B–B' complexes observed by native gel electrophoresis were identical in extracts from cells exposed to all three conditions, even though proliferation to confluence was delayed in cells treated with 5.0 mU/ml GOx (e.g., total cellular protein at 72 h was ~50% of the 10% FBS control).

Localization of hyperoxidized 2-Cys Prxs

Immunofluorescence confocal microscopy was used to localize Prx-SO_2H within C10 cells treated with various doses of GOx. In all cells, the Prx-SO_2H antibody reacted with the cell nucleus, but this signal did not correlate with the level of Prx hyperoxidation detected by immunoblotting. In cells treated with 1.0 mU/ml GOx for 3 h, immunostaining was occasionally observed in small patches at the cell periphery (Fig. 7 D), and this pattern was more obvious in cells treated with 2.5 mU/ml GOx (Fig. 7 E). At 5.0 mU/ml, GOx staining was observed in a filamentous pattern in the cell cytoplasm (Fig. 7 F). Prx-SO_2H in cytoplasmic filaments was particularly evident in cells treated with 10.0 mU/ml GOx, and at 15 mU/ml GOx, staining was prominent around the cell periphery (Fig. 7, G and H). At higher doses of GOx, the peripheral Prx-SO_2H staining pattern correlated with changes in morphology that included a considerable increase in cell diameter. A filamentous cytoplasmic staining pattern for Prx-SO_2H was not observed in asynchronous cells at any dose of GOx (Fig. 7 I and not depicted).

Ectopic expression of HA-PrxI and -PrxII and oxidant-induced arrest

Up-regulation of PrxI is thought to counteract the effects of enhanced oxidant production in tumor cells and thereby promote cell survival and proliferation (Chang et al., 2005; Park et al., 2006).

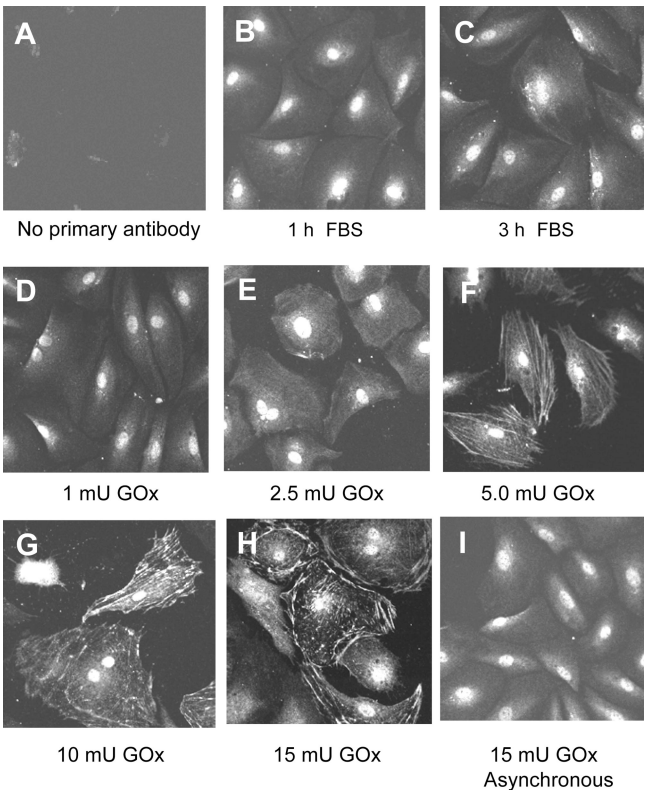

Figure 7. **Organization of cytoplasmic Prx-SO_2H in response to oxidative stress.** C10 cells were plated on coverslips and synchronized in G0 by serum deprivation. After serum stimulation for 3 h, with or without exposure to the indicated concentration of GOx (mU/ml), cells were stained for Prx-SO_2H and examined by confocal microscopy. Asynchronous C10 cells treated with GOx were used as controls.

To test the effects of Prx expression on responses to GOx, we generated expression vectors for HA-tagged PrxI, PrxII, and PrxII-ΔC, a robust mutant of PrxII that is 100-fold less sensitive to inactivation by H_2O_2 (Koo et al., 2002; Wood et al., 2003a). HA-PrxI interacts with endogenous PrxI in coimmunoprecipitation experiments, and HA-PrxI and -PrxII are hyperoxidized in response to GOx and reduced during recovery (unpublished data), indicating that HA-tagged Prxs function in peroxide metabolism in a manner similar to their endogenous counterparts. C10 cells were first transfected with expression constructs, and 24 h later the cultures were trypsinized and cells were plated at identical cell densities and synchronized by serum deprivation for 72 h as before. The transfected and serum-starved cell cultures were then treated with 5.0 mU/ml GOx as before.

In synchronized cells, immunoblotting showed HA-PrxI (Fig. 8 A, lanes 10–12) and HA-PrxII (lanes 13–15) were expressed at levels about fourfold that of their endogenous counterparts. Because of addition of the HA epitope tag and deletion of the PrxII C-terminal domain, HA-PrxII-ΔC comigrated with endogenous PrxII. As compared with untransfected cells (Fig. 8 A, lane 3) or vector controls (lane 6), expression of catalase (lane 9) and the robust PrxII-ΔC mutant (lane 18) reduced but did not eliminate Prx-SO_2H levels generated in response to GOx during a 3-h exposure, with 3 h of recovery period as before. HA-PrxI (Fig. 8 A, lane 12) and HA-PrxII (Fig. 8 A, lane 15) were hyperoxidized under these conditions and thereby increased the total cellular levels of Prx-SO_2H as measured by densitometry (Fig. 8 B). After recovery, expression of HA-PrxI or -PrxII did not reduce the levels of phospho-ERK1/2 or promote expression of cyclin D1 (Fig. 8 A). Although cells expressing catalase (Fig. 8 A, lanes 7–9) or PrxII-ΔC (Fig. 8 A, lanes 16–18) showed lower levels of total Prx-SO_2H and pERK1/2 after recovery, cells had not expressed cyclin D1 or resumed proliferation by this time. Expression of HA-PrxI or -PrxII did not affect expression of cyclin D1 in response to serum alone (Fig. 8 A, lanes 11 and 14). When cells treated with 5.0 mU/ml GOx were examined after 72 h of recovery, cells expressing HA-PrxI and -PrxII proliferated in a manner similar to vector controls, whereas cells expressing PrxII-ΔC resumed proliferation earlier during recovery (Fig. 8 C). Thus, as in serum-stimulated cells, the accumulation of Prx-SO_2H in cells overexpressing PrxI or -II was correlated with delays in cell cycle progression during recovery.

To confirm that HA-PrxII-ΔC was cytoprotective, stable cell lines were generated and treated with 5.0 mU GOx/ml continuously for 16 h. Flow cytometry showed that after 16 h ~30% of control cells exhibited a sub-G1 DNA content, whereas in comparison, ~10% of the cell population expressing HA-PrxII was detected in the sub-G1 fraction. In contrast, <0.5% of cells expressing PrxII-ΔC were detected in the dead cell fraction (unpublished data).

Discussion

The susceptibility of 2-Cys Prxs to inactivation by hyperoxidation is highly conserved in eukaryotes, inspiring the hypothesis that the Prx inactivation loop evolved to support peroxide-dependent signaling (Wood et al., 2003a). Here, we have examined the relationship between the oxidation state of PrxI and -II and transition from G0 into G1, a portion of the cell cycle known to respond to peroxide-dependent signaling (Finkel, 2003). Based on the presence of homodimers containing intersubunit

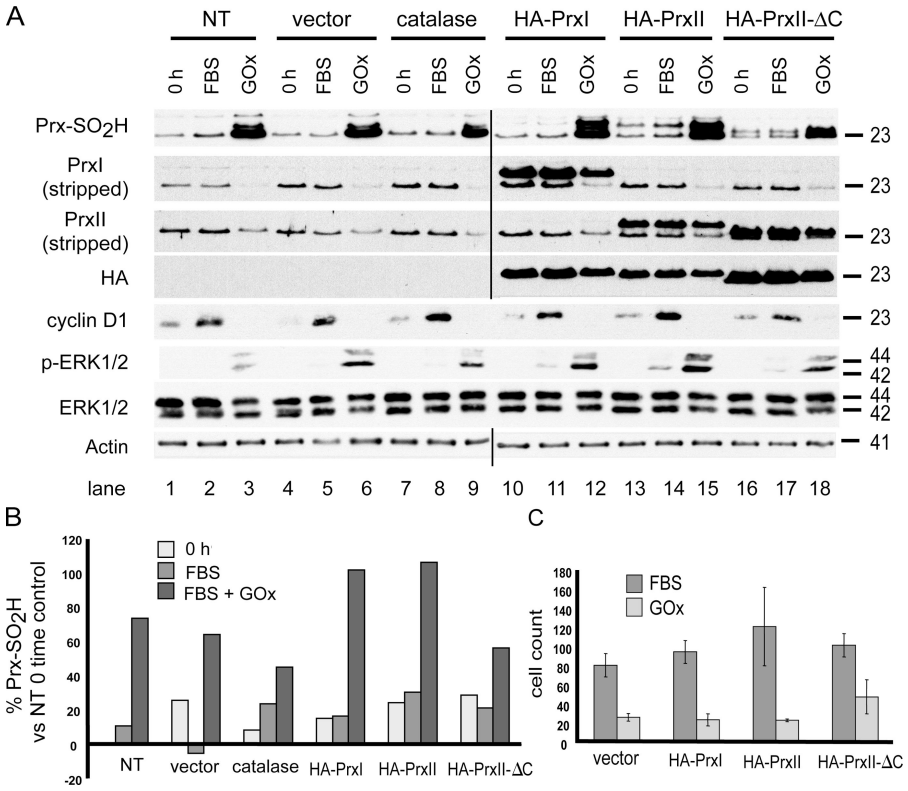

Figure 8. **Elevated expression of PrxI and -II does not prevent cell cycle arrest in response to oxidative stress.** (A) C10 cells were transfected with the indicated expression vectors or vector control, synchronized by serum deprivation, and treated with 5.0 mU/ml GOx for 3 h as in Fig. 3. After 3 h of recovery in fresh medium, cell lysates were assayed for Prx-SO_2H, HA, cyclin D1, pERK/12, and ERK1/2 levels using standard immunoblotting or for active PrxI and -II using the strip–reprobe blotting method. Nontransfected (NT) cells were included as controls for transfection. (B) Densitometry was used to quantify the total Prx-SO_2H signal for each sample presented in A. (C) After 72 h, cell numbers were determined to assess cell proliferation in cultures transfected with the indicated expression vectors. Error bars indicate mean ± SD.

disulfide bonds that are generated only during the Prx catalytic cycle, both PrxI and -II appear to metabolize H_2O_2 produced in response to serum stimulation (Fig. 5), although the source of H_2O_2, rate of catalysis, and sites of metabolism are unknown. In cells treated with DNCB (Fig. 3), which depletes cells of GSH and disrupts both Trx and GSH-dependent steps in the retroreduction cycle (Jeong et al., 2006), Prxs were sensitized to hyperoxidation by GOx. Nonetheless, in the presence of DNCB, hyperoxidation of Prxs was not observed in serum-stimulated cells at any time point, indicating that hyperoxidation of PrxI or -II may not be required during mitogenic signaling, a result that is in agreement with studies on the role of PrxII in PDGF signaling (Choi et al., 2005). Rather, our studies suggest that oligomers of hyperoxidized PrxII play a role in cell cycle arrest.

Hyperoxidized PrxI accumulated more rapidly in response to exogenous fluxes of H_2O_2 than did hyperoxidized PrxII (Fig. 3), but levels of PrxI-SO_2H did not correlate with arrest. In contrast to PrxI, cell cycle progression, arrest, and recovery were correlated with changes in the oligomeric state of PrxII. As assessed by native gel electrophoresis, PrxII existed in two complexes of ~66 kD (A–A') and ~140 kD (B–B'). As cells proliferated to confluence, both A–A' and B–B' increased in abundance and B–B' increased in complexity (Fig. 6 C). In confluent cells, the B–B' complex encompassed three distinct bands, suggesting recruitment of additional factors as cells exited the cell cycle, a matter presently under investigation.

In GOx dose-response experiments, C10 cells were able to accumulate substantial levels of hyperoxidized PrxI or -II during mitogenic signaling without marked effects on cell cycle progression. For example, exposure to 2.5 mU/ml GOx resulted in nearly complete hyperoxidation of PrxI and considerable levels of hyperoxidized PrxII, yet C10 cells were able to express cyclin D1 and proliferate. At these levels of exposure, GSH levels were unaffected, and hyperoxidized PrxI and -II were readily reduced once GOx was removed (Fig. 3). At levels of GOx that induced transient cell cycle arrest upstream of cyclin D1, but did not alter GSH levels, the B–B' PrxII complexes disappeared and hyperoxidized PrxII appeared to be incorporated into HMCs. When oxidative stress was terminated, Prx-SO_2H in HMCs was readily reduced, the B–B' complex reappeared, and cells resumed expression of cyclin D1 and cell proliferation. In contrast to the rate of hyperoxidation of PrxII seen in response to GOx (Fig. 4 B), the dose-dependent structural transitions in PrxII were abrupt (Fig. 6 B), suggesting a threshold effect for delimiting choices between cell cycle progression and arrest. Prx-dependent thresholds that regulate responses to increasing doses of H_2O_2 have been observed in yeast (Bozonet et al., 2005; Vivancos et al., 2005).

Electron microscopy shows that in vitro PrxII decamers are able to stack up on one another in an oblique fashion, forming short filaments (Harris et al., 2001). Immunostaining showed that Prx-SO_2H becomes organized in filamentous structures in the cytoplasm of serum-stimulated C10 cells (Fig. 7). Because this was not observed in asynchronous cells, recruitment of Prx-SO_2H oligomers into cytoplasmic filaments may be linked to a process active in serum-stimulated cells, such as actin stress fiber formation, or reflect acquisition of chaperone function by hyperoxidized PrxII (Moon et al., 2005). Linking the organization of PrxII to actin stress fiber formation is an attractive possibility, for actin stress fiber formation is a redox-dependent process that regulates signaling through ERK1/2 and expression of cyclin D1 (Roovers and Assoian, 2003).

Elevated expression of PrxI, PrxII, and robust mutants of these enzymes has been shown to protect cells against oxidative stress (Mu et al., 2002; Moon et al., 2004), but these studies were not conducted in synchronized cells. In our previous studies, we have observed very different responses to oxidative stress that depend on cell cycle position and cell density (Persinger et al., 2001; Yuan et al., 2003; Burch et al., 2004; Ranjan and Heintz, 2006). Differential sensitivity may be related to wiring of MAPK pathways, for JNK is not activated by H_2O_2 in synchronized C10 cells (Fig. 2), whereas it is readily activated by H_2O_2 in asynchronous C10 cells at levels that result in hyperoxidation of $<$20% of PrxI (Pantano et al., 2003; unpublished data).

In synchronized cells, a fourfold increase in expression of HA-PrxI and -PrxII relative to endogenous PrxI and -II did not reduce the level of hyperoxidized endogenous PrxI or -II in response to GOx but, rather, resulted in increased levels of total cellular Prx-SO_2H. Expression of HA-PrxI and -PrxII also did not promote cell proliferation during recovery (Fig. 8 C). Together with the GOx dose-response studies, these results indicate that oligomers of hyperoxidized Prx-SO_2H may be sensed as an anti-mitogenic signal.

Although the propensity of eukaryotic 2-Cys Prxs to be inactivated by H_2O_2 may provide a "floodgate" for permitting H_2O_2 to accumulate for redox-dependent signaling, our data provide evidence for an additional hypothesis for the conservation of the inactivation shunt in mammals. Rather than simply buffering intracellular peroxide, Prx enzymes may continuously interpret and report peroxide levels, using their redox and oligomeric states as posttranslational modifications to interface with and modulate redox-sensitive cellular events (Fig. 9). Thus, Prxs may serve as highly sensitive peroxide dosimeters that link oxidant metabolism to a variety of redox-dependent processes required for cell cycle reentry. Upon serum stimulation, these enzymes become engaged in metabolizing H_2O_2 produced in response to activation of growth factor receptors, actin stress fiber formation, cell migration, and other processes. If oxidant metabolism goes awry or the cell is exposed to threshold levels of exogenous ROS, structural transitions regulated by hyperoxidation would terminate the Prx catalytic cycle, thereby interrupting interactions with regulatory factors or disrupting redox cycling of other factors. Alternatively, PrxII-SO_2H oligomers may be sensed directly as an anti-mitogenic signal. Linking Prx hyperoxidation to cell cycle progression would allow cells to respond to perturbations in peroxide homeostasis well before depletion of GSH or disruption of the TrxR–Trx system.

It is intriguing that p53 is activated by oxidative stress and that downstream targets of p53 include factors that influence cellular redox state, including sestrins that regenerate Prx activity (Budanov et al., 2004). Retroreduction of Prxs by sulfinyl reductases is a reasonable facet of stress responses only if restoration of Prx activity contributes to recovery of activity in cell

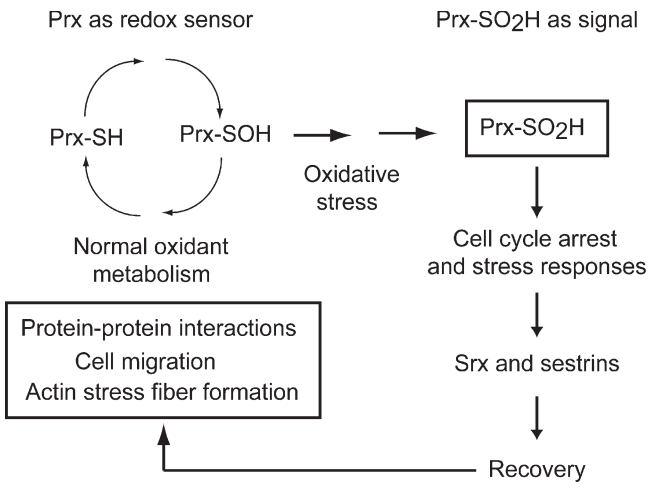

Figure 9. **A model for Prx hyperoxidation in cell signaling.** Prxs may serve as dosimeters for redox-dependent signaling events, with structural transitions induced by hyperoxidation disrupting interactions with regulatory factors or modulating other redox-dependent processes, such as actin stress fiber formation. In addition, Prx-SO_2H oligomers may be directly recognized as a signal that warns cells of perturbations in oxidant metabolism and thereby contribute to stress responses that mediate oxidant-induced cell cycle arrest.

signaling pathways, for degradation by the proteasome would be equally effective in ridding cells of hyperoxidized Prxs. Hence, 2-Cys Prxs may provide an exquisitely sensitive, widely distributed, and dose-dependent "smoke alarm" for alerting cells to oxidative stress.

Materials and methods

Cell culture, cell cycle synchronization, and oxidant exposure

C10 mouse lung epithelial cells (Malkinson et al., 1997) were cultured, synchronized, and stimulated with serum as described previously (Burch et al., 2004). For oxidant exposures, recombinant GOx (Roche) in 10 mM phosphate buffer, pH 7.4, was diluted in medium immediately before use. Levels of H_2O_2 generated by GOx in complete medium were determined as described previously (van der Vliet et al., 1997). DNCB (Sigma-Aldrich) was dissolved in DMSO and used at a final concentration of 5 μM. For growth curves, cells were plated in duplicate in 6-well dishes and treated as described (see Results) before trypsinization and counting with a hemocytometer.

Lysis buffers

Cell extracts were prepared with NP-40 lysis buffer (150 mM NaCl, 1.0% NP-40, 50 mM Tris, pH 8.0, 1 μg/ml leupeptin, 1 μg/ml aprotinin, 1 mM NaF, 1 mM $NaVO_3$, and 1 mM PMSF) or passive lysis buffer (Promega) as noted. At harvest, cells in 60-mM dishes were washed once with cold PBS, pH 7.4, 100 μl of lysis buffer were added, and lysates were collected by scraping with a rubber policeman. The insoluble fraction was pelleted by centrifugation in a microfuge for 5 min, and the protein concentration of the soluble fraction was determined using a protein assay (Bio-Rad Laboratories).

Electrophoresis and immunoblotting

For reducing SDS-PAGE, lysates were diluted 1:5 with 5× sample buffer (10% SDS, 500 mM DTT, 300 mM Tris, pH 6.8, 0.05% bromophenol blue, and 50% glycerol), heated at 95°C for 5 min before resolution on 12% SDS-PAGE gels. Nonreducing SDS-PAGE was performed in the same manner, except that DTT was omitted from sample buffer. For native-PAGE, NP-40 lysates were diluted in 5× sample buffer without DTT or SDS and resolved on 8% polyacrylamide gels without SDS. Under all conditions, proteins were transferred onto Immobilon-P PVDF (Millipore). Membranes were blocked with 5% nonfat milk in TBS/T (25 mM Tris, pH 8, 150 mM NaCl, and 0.1% Tween-20) and incubated with primary antibodies diluted in 5% milk in TBS/T. Reactive proteins were visualized by HRP-conjugated secondary antibodies (GE Healthcare) and chemiluminescence using Western Lightning ECL (PerkinElmer).

Total levels of PrxI and -II were determined using SDS-PAGE and immunoblotting conditions as described previously (Burch et al., 2004). For assessing relative levels of PrxI and -II that were not hyperoxidized, blots were first probed for Prx-SO_2H using anti-PrxSO_3 antibody (Lab Frontier) and then stripped at 50°C for 15 min in 62.5 mM Tris, pH 6.8, 2% SDS, and 100 mM β-mercaptoethanol. Stripped blots were washed several times with TBS/T, blocked in 5% nonfat milk in TBS/T for 30 min, and reprobed with anti-PrxI or anti-PrxII antibody. In contrast to probing for Prx-SO_2H first, probing for PrxI or -II before stripping and reprobing with Prx-SO_2H antibody did not influence detection of Prx-SO_2H isoforms.

Antibodies

Antibodies for PrxI (LF-PA0001), PrxII (LF-PA0007), and Prx-SO_2H/SO_3 (LF-PA0004) were obtained from Lab Frontier. Antibodies to ERK1/2 (9102), phospho-ERK1/2 (9101), and phospho-JNK (9251) were obtained from Cell Signaling Technologies. Anti-phosphotyrosine mouse monoclonal 4G10 was purchased from Upstate Cell Signaling Solutions, anti–cyclin D1 (sc-450) was purchased from Santa Cruz Biotechnology, Inc., and anti-actin from Sigma-Aldrich. Mouse monoclonal anti-HA 12CA5 was a gift from E. Harlow (Harvard University, Cambridge, MA).

Plasmid construction and transfection

Full-length coding sequences for human PrxI and -II were recovered with BamHI ends from pET-17 (Novagen) vectors (Kang et al., 1998) using PCR and the following primer sets: PrxI forward, 5′-cgcggatccatgtcttcaggaaatg-3′; PrxI reverse, 5′-cgcggatcctcacttctgcttgg-3′; PrxII forward, 5′-cgcggatccatggcctccggtaacg-3′; PrxII reverse, 5′-gcgggatccctaattgtgtttggag-3′. PrxII-ΔC was generated from a previously described pET-19 (Novagen) PrxII construct (Jönsson et al., 2005) by introducing a stop codon at D188 using the QuikChange site-mutagenesis kit (Stratagene) with the following primers: forward, 5′-GACACGATTAAGCCCAACGTGTAGGACAGCAAGGAATATTTC-3′; reverse, 5′-GAAATATTCCTTGCTGTCCTACACGTTGGGCTTAATCGTGTC-3′. PrxII-ΔC was subcloned from the PrxII pET-19 vector using the PrxII primers listed. PCR products were cloned first using topo-TA cloning vector pCR2.1 (Invitrogen). Positive clones were digested with BamHI, and fragments were subcloned into pCMV-HA to introduce an N-terminal HA epitope tag. The pZeoSV-catalase expression vector (Arnold et al., 2001) was a gift from D. Lambeth (Emory University, Atlanta, GA). Expression constructs were propagated in DH5α cells and prepared for transfection by alkaline lysis and sedimentation to equilibrium in CsCl. Asynchronous C10 cells at 70% confluence in 60-mm plates were cotransfected with Prx expression plasmids and an EGFP expression vector (pEGFP-N2; CLONTECH Laboratories, Inc.) using Lipofectamine 2000 (Invitrogen) according to manufacturer's protocols. Based on EGFP expression, transfection efficiency was routinely >70%.

GSH measurements

C10 cells were lysed in 1% Triton, 50 mM Hepes, 250 mM NaCl, 10% glycerol, 1.5 mM $MgCl_2$, 1 mM PMSF, 1 mM EGTA, 2 mM Na_3VO_4, 10 μg/ml aprotinin, and 10 μg/ml leupeptin, pH 7.4. GSH was measured as previously described with some modifications (van der Vliet et al., 1998). In brief, samples were mixed 1:1 with 2 mM monobromobimane (Thiolyte; Calbiochem) in 50 mM *N*-ethylmorpholine, pH 8.0, and incubated at RT for 5 min in the dark. Trichloroacetic acid was added to the reaction mixture to a final concentration of 5%. Samples were centrifuged at 3,000 *g* for 5 min, and supernatants were injected onto a Waters Symmetree C-18 column (150 × 4.5 mm). The GSH-monobromobimane adduct was eluted with 10% CH_3CN/0.25% glacial acetic acid and detected by fluorescence emission of 480 nm after excitation at 395 nm.

Confocal microscopy

C10 cells were plated on glass coverslips in 100-mm tissue culture dishes, synchronized or allowed to grow asynchronously to 70% confluence, and treated as indicated. Coverslips were rinsed with PBS, fixed with 3% paraformaldehyde for 15 min at RT, and washed several times with PBS, and cells were permeabilized with 0.1% Triton X-100 in PBS for 15 min at RT. After gentle washing, coverslips were blocked for 1 h at RT with 10% normal goat serum in PBS and incubated with 1 μg/ml Prx-SO_2H antibody in PBS with 1% BSA overnight at 4°C. Alexa Fluor 594 (Invitrogen) conjugated goat anti–rabbit secondary antibody at 1 μg/ml in PBS was added for 25 min at RT in the dark. Coverslips were mounted on slides, and

images were generated at RT using a confocal scanning laser microscope (MRC 1024 ES; Bio-Rad Laboratories) on a stand (BX50; Olympus), using a 40× Plan-Apo lens (Olympus) with a 0.95 NA and a correction collar. Digital images were collected with Laser Sharp Capture Software (Bio-Rad Laboratories) and processed as black-and-white images. Contrast was adjusted using Photoshop (Adobe).

We thank Peter Burch and Anne Loonen for measuring the generation of H_2O_2 in medium by GOx and Yvonne Janssen-Heininger and Todd Lowther for useful discussions.

This work was supported by grants from the National Heart, Lung, and Blood Institute (P01 HL67004) and General Medical Sciences (R01 GM074204). T.J. Phalen was supported by an National Institute of Environmental Health Sciences environmental pathology training grant (T32 ES007122).

Submitted: 2 June 2006
Accepted: 30 October 2006

References

Arner, E.S., M. Bjornstedt, and A. Holmgren. 1995. 1-Chloro-2,4-dinitrobenzene is an irreversible inhibitor of human thioredoxin reductase. Loss of thioredoxin disulfide reductase activity is accompanied by a large increase in NADPH oxidase activity. *J. Biol. Chem.* 270:3479–3482.

Arnold, R.S., J. Shi, E. Murad, A.M. Whalen, C.Q. Sun, R. Polavarapu, S. Parthasarathy, J.A. Petros, and J.D. Lambeth. 2001. Hydrogen peroxide mediates the cell growth and transformation caused by the mitogenic oxidase Nox1. *Proc. Natl. Acad. Sci. USA.* 98:5550–5555.

Baty, J.W., M.B. Hampton, and C.C. Winterbourn. 2005. Proteomic detection of hydrogen peroxide-sensitive thiol proteins in Jurkat cells. *Biochem. J.* 389:785–795.

Biteau, B., J. Labarre, and M.B. Toledano. 2003. ATP-dependent reduction of cysteine-sulphinic acid by *S. cerevisiae* sulphiredoxin. *Nature.* 425:980–984.

Bozonet, S.M., V.J. Findlay, A.M. Day, J. Cameron, E.A. Veal, and B.A. Morgan. 2005. Oxidation of a eukaryotic 2-Cys peroxiredoxin is a molecular switch controlling the transcriptional response to increasing levels of hydrogen peroxide. *J. Biol. Chem.* 280:23319–23327.

Budanov, A.V., A.A. Sablina, E. Feinstein, E.V. Koonin, and P.M. Chumakov. 2004. Regeneration of peroxiredoxins by p53-regulated sestrins, homologs of bacterial AhpD. *Science.* 304:596–600.

Burch, P.M., and N.H. Heintz. 2005. Redox regulation of cell-cycle re-entry: cyclin D1 as a primary target for the mitogenic effects of reactive oxygen and nitrogen species. *Antioxid. Redox Signal.* 7:741–751.

Burch, P.M., Z. Yuan, A. Loonen, and N.H. Heintz. 2004. An extracellular signal-regulated kinase 1- and 2-dependent program of chromatin trafficking of c-Fos and Fra-1 is required for cyclin D1 expression during cell cycle reentry. *Mol. Cell. Biol.* 24:4696–4709.

Chang, J.W., S.H. Lee, J.Y. Jeong, H.Z. Chae, Y.C. Kim, Z.Y. Park, and Y.J. Yoo. 2005. Peroxiredoxin-I is an autoimmunogenic tumor antigen in non-small cell lung cancer. *FEBS Lett.* 579:2873–2877.

Chang, T.S., W. Jeong, S.Y. Choi, S. Yu, S.W. Kang, and S.G. Rhee. 2002. Regulation of peroxiredoxin I activity by Cdc2-mediated phosphorylation. *J. Biol. Chem.* 277:25370–25376.

Chang, T.S., W. Jeong, H.A. Woo, S.M. Lee, S. Park, and S.G. Rhee. 2004. Characterization of mammalian sulfiredoxin and its reactivation of hyperoxidized peroxiredoxin through reduction of cysteine sulfinic acid in the active site to cysteine. *J. Biol. Chem.* 279:50994–51001.

Choi, M.H., I.K. Lee, G.W. Kim, B.U. Kim, Y.H. Han, D.Y. Yu, H.S. Park, K.Y. Kim, J.S. Lee, C. Choi, et al. 2005. Regulation of PDGF signalling and vascular remodelling by peroxiredoxin II. *Nature.* 435:347–353.

Egler, R.A., E. Fernandes, K. Rothermund, S. Sereika, N. de Souza-Pinto, P. Jaruga, M. Dizdaroglu, and E.V. Prochownik. 2005. Regulation of reactive oxygen species, DNA damage, and c-Myc function by peroxiredoxin 1. *Oncogene.* 24:8038–8050.

Finkel, T. 2003. Oxidant signals and oxidative stress. *Curr. Opin. Cell Biol.* 15:247–254.

Forman, H.J., J.M. Fukuto, and M. Torres. 2004. Redox signaling: thiol chemistry defines which reactive oxygen and nitrogen species can act as second messengers. *Am. J. Physiol. Cell Physiol.* 287:C246–C256.

Gabbita, S.P., K.A. Robinson, C.A. Stewart, R.A. Floyd, and K. Hensley. 2000. Redox regulatory mechanisms of cellular signal transduction. *Arch. Biochem. Biophys.* 376:1–13.

Harris, J.R., E. Schroder, M.N. Isupov, D. Scheffler, P. Kristensen, J.A. Littlechild, A.A. Vagin, and U. Meissner. 2001. Comparison of the decameric structure of peroxiredoxin-II by transmission electron microscopy and X-ray crystallography. *Biochim. Biophys. Acta.* 1547:221–234.

Immenschuh, S., and E. Baumgart-Vogt. 2005. Peroxiredoxins, oxidative stress, and cell proliferation. *Antioxid. Redox Signal.* 7:768–777.

Jang, H.H., S.Y. Kim, S.K. Park, H.S. Jeon, Y.M. Lee, J.H. Jung, S.Y. Lee, H.B. Chae, Y.J. Jung, K.O. Lee, et al. 2006. Phosphorylation and concomitant structural changes in human 2-Cys peroxiredoxin isotype I differentially regulate its peroxidase and molecular chaperone functions. *FEBS Lett.* 580:351–355.

Jeong, W., S.J. Park, T.S. Chang, D.Y. Lee, and S.G. Rhee. 2006. Molecular mechanism of the reduction of cysteine sulfinic acid of peroxiredoxin to cysteine by mammalian sulfiredoxin. *J. Biol. Chem.* 281:14400–14407.

Jönsson, T.J., M.S. Murray, L.C. Johnson, L.B. Poole, and W.T. Lowther. 2005. Structural basis for the retroreduction of inactivated peroxiredoxins by human sulfiredoxin. *Biochemistry.* 44:8634–8642.

Kang, S.W., H.Z. Chae, M.S. Seo, K. Kim, I.C. Baines, and S.G. Rhee. 1998. Mammalian peroxiredoxin isoforms can reduce hydrogen peroxide generated in response to growth factors and tumor necrosis factor-alpha. *J. Biol. Chem.* 273:6297–6302.

Karin, M., and E. Shaulian. 2001. AP-1: linking hydrogen peroxide and oxidative stress to the control of cell proliferation and death. *IUBMB Life.* 52:17–24.

Koo, K.H., S. Lee, S.Y. Jeong, E.T. Kim, H.J. Kim, K. Kim, K. Song, and H.Z. Chae. 2002. Regulation of thioredoxin peroxidase activity by C-terminal truncation. *Arch. Biochem. Biophys.* 397:312–318.

Malkinson, A.M., L.D. Dwyer-Nield, P.L. Rice, and D. Dinsdale. 1997. Mouse lung epithelial cell lines—tools for the study of differentiation and the neoplastic phenotype. *Toxicology.* 123:53–100.

Moon, E.Y., Y.H. Han, D.S. Lee, Y.M. Han, and D.Y. Yu. 2004. Reactive oxygen species induced by the deletion of peroxiredoxin II (PrxII) increases the number of thymocytes resulting in the enlargement of PrxII-null thymus. *Eur. J. Immunol.* 34:2119–2128.

Moon, J.C., Y.S. Hah, W.Y. Kim, B.G. Jung, H.H. Jang, J.R. Lee, S.Y. Kim, Y.M. Lee, M.G. Jeon, C.W. Kim, et al. 2005. Oxidative stress-dependent structural and functional switching of a human 2-Cys peroxiredoxin isotype II that enhances HeLa cell resistance to H2O2-induced cell death. *J. Biol. Chem.* 280:28775–28784.

Mu, Z.M., X.Y. Yin, and E.V. Prochownik. 2002. Pag, a putative tumor suppressor, interacts with the Myc Box II domain of c-Myc and selectively alters its biological function and target gene expression. *J. Biol. Chem.* 277:43175–43184.

Pantano, C., P. Shrivastava, B. McElhinney, and Y. Janssen-Heininger. 2003. Hydrogen peroxide signaling through tumor necrosis factor receptor 1 leads to selective activation of c-Jun N-terminal kinase. *J. Biol. Chem.* 278:44091–44096.

Park, J.H., Y.S. Kim, H.L. Lee, J.Y. Shim, K.S. Lee, Y.J. Oh, S.S. Shin, Y.H. Choi, K.J. Park, R.W. Park, and S.C. Hwang. 2006. Expression of peroxiredoxin and thioredoxin in human lung cancer and paired normal lung. *Respirology.* 11:269–275.

Parsonage, D., D.S. Youngblood, G.N. Sarma, Z.A. Wood, P.A. Karplus, and L.B. Poole. 2005. Analysis of the link between enzymatic activity and oligomeric state in AhpC, a bacterial peroxiredoxin. *Biochemistry.* 44:10583–10592.

Persinger, R.L., W.M. Blay, N.H. Heintz, D.R. Hemenway, and Y.M. Janssen-Heininger. 2001. Nitrogen dioxide induces death in lunch epithelial cells in a density-dependent manner. *Am. J. Respir. Cell Mol. Biol.* 24:583–590.

Ranjan, P., and N. Heintz. 2006. S-phase arrest by reactive nitrogen species is bypassed by okadaic acid, an inhibitor of protein phosphatases PP1/PP2. *Free Radic. Biol. Med.* 15: 247–249.

Ranjan, P., V. Anathy, P.M. Burch, K. Weirather, J.D. Lambeth, and N.H. Heintz. 2006. Redox-dependent expression of cyclin D1 and cell proliferation by Nox1 in mouse lung epithelial cells. *Antioxid. Redox Signal.* 8:1447–1459.

Rhee, S.G., S.W. Kang, W. Jeong, T.S. Chang, K.S. Yang, and H.A. Woo. 2005. Intracellular messenger function of hydrogen peroxide and its regulation by peroxiredoxins. *Curr. Opin. Cell Biol.* 17:183–189.

Roovers, K., and R.K. Assoian. 2003. Effects of rho kinase and actin stress fibers on sustained extracellular signal-regulated kinase activity and activation of G(1) phase cyclin-dependent kinases. *Mol. Cell. Biol.* 23:4283–4294.

Schwartz, M.A., and R.K. Assoian. 2001. Integrins and cell proliferation: regulation of cyclin-dependent kinases via cytoplasmic signaling pathways. *J. Cell Sci.* 114:2553–2560.

Tu, B.P., A. Kudlicki, M. Rowicka, and S.L. McKnight. 2005. Logic of the yeast metabolic cycle: temporal compartmentalization of cellular processes. *Science.* 310:1152–1158.

van der Vliet, A., J.P. Eiserich, B. Halliwell, and C.E. Cross. 1997. Formation of reactive nitrogen species during peroxidase-catalyzed oxidation of nitrite. A potential additional mechanism of nitric oxide-dependent toxicity. *J. Biol. Chem.* 272:7617–7625.

van der Vliet, A., P.A. Hoen, P.S. Wong, A. Bast, and C.E. Cross. 1998. Formation of S-nitrosothiols via direct nucleophilic nitrosation of thiols by peroxynitrite with elimination of hydrogen peroxide. *J. Biol. Chem.* 273:30255–30262.

Vivancos, A.P., E.A. Castillo, B. Biteau, C. Nicot, J. Ayte, M.B. Toledano, and E. Hidalgo. 2005. A cysteine-sulfinic acid in peroxiredoxin regulates H_2O_2-sensing by the antioxidant Pap1 pathway. *Proc. Natl. Acad. Sci. USA.* 102:8875–8880.

Wen, S.T., and R.A. Van Etten. 1997. The PAG gene product, a stress-induced protein with antioxidant properties, is an Abl SH3-binding protein and a physiological inhibitor of c-Abl tyrosine kinase activity. *Genes Dev.* 11:2456–2467.

Wood, Z.A., L.B. Poole, R.R. Hantgan, and P.A. Karplus. 2002. Dimers to doughnuts: redox-sensitive oligomerization of 2-cysteine peroxiredoxins. *Biochemistry.* 41:5493–5504.

Wood, Z.A., L.B. Poole, and P.A. Karplus. 2003a. Peroxiredoxin evolution and the regulation of hydrogen peroxide signaling. *Science.* 300:650–653.

Wood, Z.A., E. Schroder, J. Robin Harris, and L.B. Poole. 2003b. Structure, mechanism and regulation of peroxiredoxins. *Trends Biochem. Sci.* 28:32–40.

Xiao, N., G. Du, and M.A. Frohman. 2005. Peroxiredoxin II functions as a signal terminator for H_2O_2-activated phospholipase D1. *FEBS J.* 272:3929–3937.

Yuan, Z., H. Schellekens, L. Warner, Y. Janssen-Heininger, P. Burch, and N.H. Heintz. 2003. Reactive nitrogen species block cell cycle re-entry through sustained production of hydrogen peroxide. *Am. J. Respir. Cell Mol. Biol.* 28:705–712.

Yuan, Z., D.J. Taatjes, B.T. Mossman, and N.H. Heintz. 2004. The duration of nuclear extracellular signal-regulated kinase 1 and 2 signaling during cell cycle reentry distinguishes proliferation from apoptosis in response to asbestos. *Cancer Res.* 64:6530–6536.